High-resolution isotope stratigraphy of the Lower Ordovician St. George Group of western Newfoundland, Canada: implications for global correlation

Karem Azmy and Denis Lavoie

Abstract: The Lower Ordovician St. George Group of western Newfoundland consists mainly of shallow-marine-platform carbonates (~500 m thick). It is formed, from bottom to top, of the Watts Bight, Boat Harbour, Catoche, and Aguathuna formations. The top boundary of the group is marked by the regional St. George Unconformity. Outcrops and a few cores from western Newfoundland were sampled at high resolution and the extracted micritic materials were investigated for their petrographic and geochemical criteria to evaluate their degree of preservation. The $\delta^{13}C$ and $\delta^{18}O$ values of well-preserved micrite microsamples range from –4.2‰ to 0‰ (VPDB) and from –11.3‰ to –2.9‰ (VPDB), respectively. The $\delta^{13}C_{carb}$ profile of the St. George Group carbonates reveals several negative shifts, which vary between ~2‰ and 3‰ and are generally associated with unconformities–disconformities or thin shale interbeds, thus reflecting the effect of or link with significant sea-level changes. The St. George Unconformity is associated with a negative $\delta^{13}C_{carb}$ shift (~2‰) on the profile and correlated with major lowstand (around the end of Arenig) on the local sea-level reconstruction and also on those from the Baltic region and central Australia, thus suggesting that the St. George Group Unconformity might have likely had an eustatic component that contributed to the development–enhancement of the paleomargin. Other similar $\delta^{13}C_{carb}$ shifts have been recorded on the St. George profile, but it is hard to evaluate their global extension due to the low resolution of the documented global Lower Ordovician (Tremadoc – middle Arenig) $\delta^{13}C_{carb}$ profile.

Résumé : Le Groupe de St. George (Ordovicien inférieur) de l'ouest de Terre-Neuve comprend surtout des carbonates de plate-forme marine peu profonde (épaisseur ~500 m). De la base au sommet, il comprend les formations suivantes : Watts Bight, Boat Harbour, Catoche et Aguathuna. La limite supérieure du groupe est marquée par la discordance régionale de St. George. Des affleurements et quelques carottes provenant de l'ouest de Terre-Neuve ont été échantillonnés à haute résolution et les roches micritiques extraites ont été étudiées pour leurs critères pétrographiques et géochimiques afin d'évaluer leur degré de préservation. Les valeurs $\delta^{13}C$ et $\delta^{18}O$ de micro-échantillons de micrites bien préservées variaient respectivement entre –4,2 ‰ à 0 ‰ « VPDB » et entre –11,3 ‰ à –2,9 ‰ (VPDB). Le profil $\delta^{13}C_{carb}$ des carbonates du Groupe de St. George montre plusieurs changements à des valeurs négatives; ces changements varient entre ~2 ‰ à 3 ‰ et ils sont généralement associés à des discordances ou à de minces interlits de shale, reflétant ainsi l'effet des changements importants de niveau de la mer ou ayant un lien avec ces changements. La discordance de St. George est associée à un changement négatif $\delta^{13}C_{carb}$ (~2 ‰) du profil et elle est corrélée à un important bas niveau dans une reconstruction locale du niveau de la mer (vers la fin de l'Arenigien) ainsi qu'à des bas niveaux dans des régions de la Baltique et du centre de l'Australie, portant ainsi à croire que la discordance du Groupe de St. George avait une composante eustatique qui a contribué au développement – rehaussement de la paléobordure.

[Traduit par la Rédaction]

Introduction

The stable isotope signatures encrypted in preserved marine carbonates have been successfully utilized to understand the evolution of the Earth's system and correlation of sedimentary sequences from different depositional settings and paleolandmasses (e.g., Veizer et al. 1999; Halverson et al. 2005; Immenhauser et al. 2008). For some successions, the lack of high-resolution biostratigraphy makes chemostratigraphy a potential tool for refining correlations. The reconstructed isotope profiles, particularly those of carbon isotopes, can be also used for better understanding geological processes and paleo-oceanographic events (e.g., Veizer et al. 1999).

Sea-level changes at the southern shallow-marine paleomargin of Laurentia during the Early Ordovician likely had an impact on organic productivity and oxidation of buried organic matter at the lower margin, which was reflected particularly in the C-isotopic composition of the deposited marine carbonates. The low-resolution of the global Early Ordovician carbon-isotope profile (cf. Qing and Veizer

Received 11 March 2009. Accepted 30 June 2009. Published on the NRC Research Press Web site at cjes.nrc.ca on 7 August 2009.

Paper handled by Associate Editor G. Dix.

K. Azmy.[1] Department of Earth Sciences, Memorial University of Newfoundland, St. John's, NL A1B 3X5 Canada.
D. Lavoie. Geological Survey of Canada, GSC-Q, Natural Resources Canada, 490 de la Couronne, Quebec, QC G1K 9A9, Canada.

[1]Corresponding author (e-mail: kazmy@mun.ca).

Fig. 1. Map showing the approximate locations of the study areas in western Newfoundland, Canada (modified from Zhang et al. 2004).

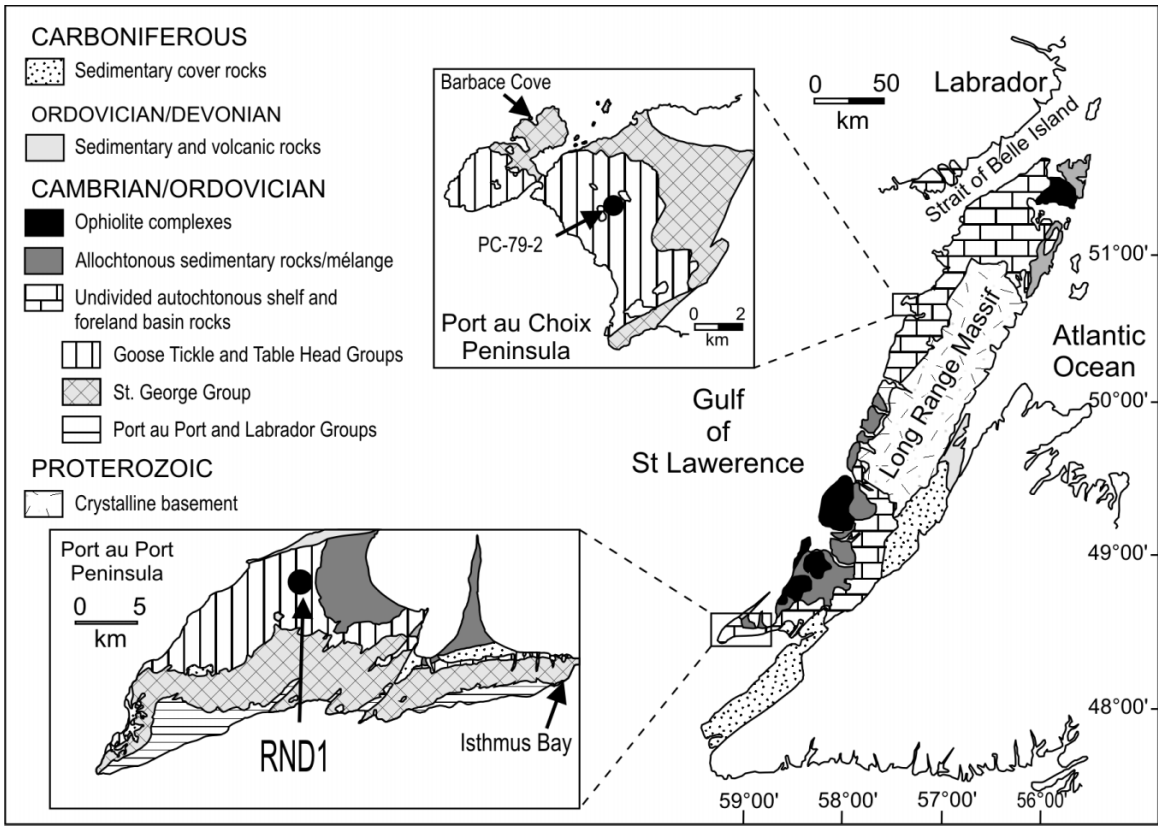

Table 1. Summary of the lithostratigraphy of the St. George Group, Newfoundland. Detailed description in Knight et al. (2007, 2008).

Formation	Lithology
Aguathuna	~70 m thick; dolomitized peritidal carbonates; burrow mottled dolostone, dolomicrite, and stromatolitic dolostones; rare thin shale beds; skeletal peloidal, oolitic and oncolitic grainstones; peloidal wackestones and packstones; microbial (stromatolitic) lime mudstones
Catoche	Up to 160 m thick; mainly limestones in the lower part (~120 m) and dolostones in the upper part (~40 m); bedded gray carbonates; bioturbated at times; skeletal garinstone to peloidal wackestone and a packstone; microbial lime mudstones
Boat Harbour	Up to 170 m thick; lower member (~44 m) of partially dolomitized grainstones, wackestones, thrombolites, and laminated microbial mats; mainly microbial lime mustone and stromatolitic mounds but rarely grainstones in the middle member (~70 m) between the lower disconformity and the overlying Boat Harbour disconformity; peloidal grainstone to microbial lime mudstones in the upper member (~52 m, Barbace Cove Member)
Watts Bight	~70 m thick; partially dolomitized microbial lime mudstone in the lower part (~33 m); burrowed grainstone in the middle part (~25 m); microbial lime mudstone in the upper part (~11 m)

1994; Veizer et al. 1999; Shields et al. 2003) makes the high-resolution $\delta^{13}C$ variations of the investigated St. George Group carbonates a potential reliable database for the reconstruction of a refined regional (Laurentian) profile, which might also allow for possible global correlation (cf. Immenhauser et al. 2008; Bergström et al. 2009).

In the current study, we investigate the major $\delta^{13}C$ variations in the St. George Group carbonates (Lower Ordovician, Tremadoc – early Arenig) in an attempt to establish a reliable C-isotope stratigraphic profile, which could be utilized for high-resolution correlations in the area and possibly beyond.

Geologic setting

The lower Paleozoic sediments in western Newfoundland (Fig. 1) were intensively affected by complex orogenic events. The Laurentian plate broke from Rodinia through an active rifting event ~570–550 Ma (Cawood et al. 2001). After rifting, in Early Cambrian, a preplatform shelf developed and was later covered by clastics (James et al. 1989). As the continental margin was slowly established during an early drift episode, a major sea transgression flooded the Laurentia margin and resulted in a thick carbonate-platform succession (Wilson et al. 1992; Knight et al. 2007, 2008 and references therein). During Middle to Late Cambrian, the platform deposits were dominated by high-energy carbonates of the Port au Port Group. These carbonates evolved into the Early to earliest Middle Ordovician low-energy carbonates of the St. George Group (cf. Knight et al. 2007, 2008). Lithospheric depressions from sediment surcharge in Taconian fore arcs resulted in distal lithospheric upwarding and

Fig. 2. Diagram showing the stratigraphic framework of the St. George Group (after Knight et al. 2007, 2008), sea-level changes in the Laurentian Basin during the deposition of investigated sequence (Early to early Middle Ordovician), and the biozonation scheme (modified from Boyce and Stouge 1997; Zhang and Barnes 2004).

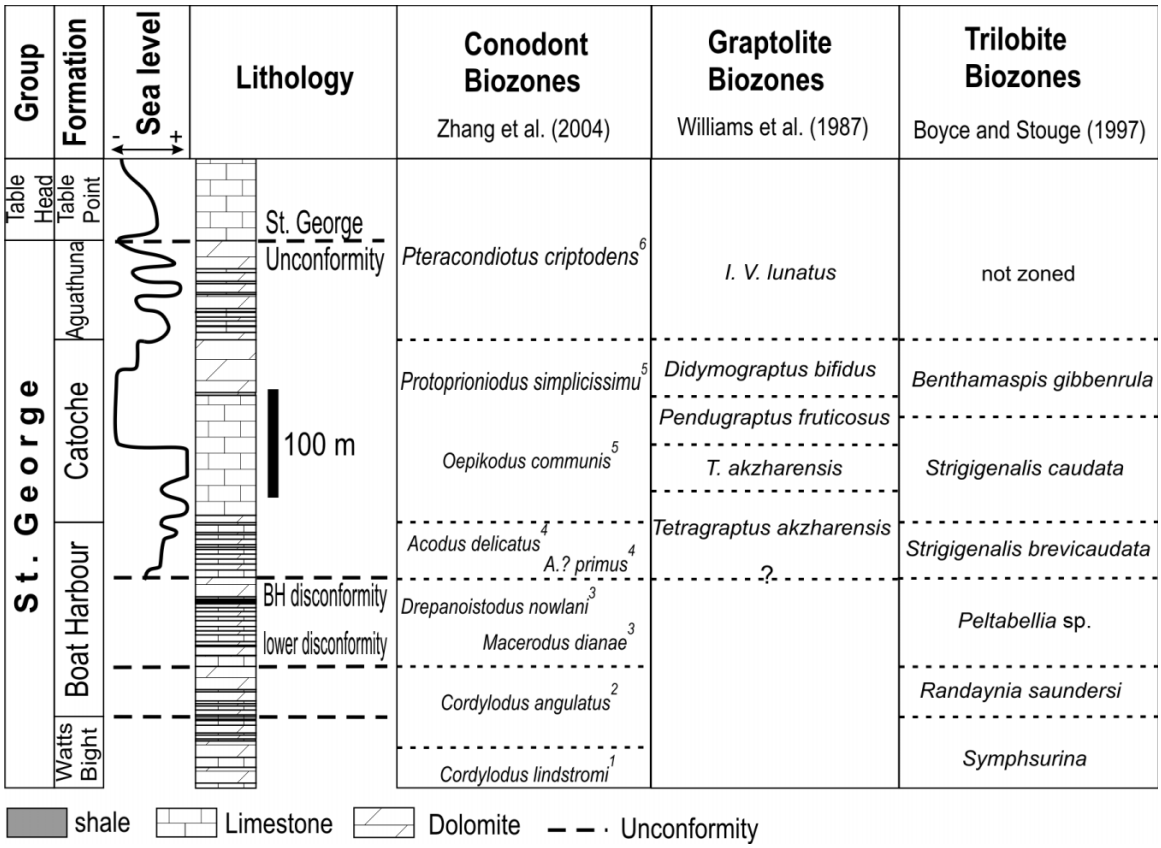

rapid sweeping of a tectonic peripheral bulge on the margin in earliest Middle Ordovician (Jacobi 1981; Knight et al. 1991). The migration of that lithospheric high led to compression, block faulting, uplift, and erosion of the St. George carbonate platform and the development of the regional St. George Unconformity, which leaves the first physical imprint of the transition from a passive margin to a foreland basin (Mussman and Read 1986; Knight et al. 1991, 2007; Lavoie 1994; Cooper et al. 2001). The transition was thus associated with regional tectonic instability that overlapped with falling sea level. The interplay of tectonism and eustatic sea-level changes was assumed to be responsible for the relative sea-level fall and the development of the St. George Unconformity (Knight et al. 1991). A later tectonically driven local sea-level rise accommodated the deposition of the younger Table Head Group (Stenzel et al. 1990; Knight et al. 1991, 2007).

Lithostratigraphy and biostratigraphy

Lower Paleozoic successions deposited on Laurentia shallow-marine-platform margin are characterized by a thick Middle Cambrian to lower Middle Ordovician carbonate bank. The lithostratigraphy of the St. George Group has been documented, discussed in detail, and refined by several authors (e.g., Pratt and James 1986; Knight and James 1987; Knight 1991; Baker and Knight 1993; Cooper et al. 2001; Knight et al. 2007, 2008). The lithostratigraphic framework is briefly summarized in Table 1, since the current investigation is mainly focused on the chemostratigraphy of the group. The St. George Group consists of Early Ordovician (Tremadoc–Arenig) platform carbonates (500 m thick), which, from bottom to top, include the Watts Bight, Boat Harbour, Catoche, and Aguathuna formations (Table 1). The upper boundary of the St. George Group (Aguathuna – Table Point formations contact) is marked by the major regional St. George Group Unconformity (Fig. 2). The St. George Group can be divided into two sedimentary megacycles separated by the Boat Harbour Disconformity (Fig. 2). Each megacycle is characterized by a large-scale transgressive–regressive succession that resulted in stacking of lower peritidal, middle subtidal, and upper peritidal units (Knight and James 1987; Knight et al. 2007, 2008). The Boat Harbour Formation is divided into three members separated by two disconformities (Knight et al. 2008), the stratigraphically higher Boat Harbour Disconformity and an unnamed lower disconformity (Fig. 2). Both disconformities are associated with paleokarst and marked by micro and macro faunal changes (Knight and James 1987; Knight 1991; Ji and Barnes 1993; Boyce and Stouge 1997; Knight et al. 2007, 2008). The upper member, the Barbace Cove Member (Knight and James 1987; Knight 1991), is the initial part of an Arenig transgressive event that onlapped the upper disconformity at a time of global eustatic sea-level rise onto and across the Laurentian margin (upper mega-

Table 2. Summary of statistics of isotopic and trace element geochemical compositions of the investigated St. George Group carbonates.

	$CaCO_3$%	$MgCO_3$%	Mn (ppm)	Sr (ppm)	$\delta^{18}O$‰ VPDB	$\delta^{13}C$‰ VPDB	$\delta^{13}C_{organic}$‰ VPDB	TOC (%)	$\Delta\delta$	Carbonate (%)	Mn/Sr
All formations											
n	95	95	95	95	167	167	100	100	98	98	95
Average	79.3	20.7	170	220	–6.9	–1.7	–27.6	0.3	26.0	93.0	1.38
Standard deviation	18.4	18.4	169	130	1.7	0.8	2.2	0.5	2.5	7.2	1.62
Maximum	99.4	47.1	836	653	–2.9	0.0	–22.1	3.3	35.0	99.7	7.72
Minimum	52.9	0.6	26	27	–11.3	–4.2	–35.1	0.0	19.7	46.1	0.08
Aguathuna											
n	23	23	23	23	38	38	22	22	22	22	23
Average	70.4	29.6	232	164	–4.9	–1.5	–27.7	0.1	26.2	92.9	2.35
Standard deviation	21.0	21.0	220	134	1.5	0.6	1.0	0.1	1.0	6.5	2.32
Maximum	99.4	47.0	836	653	–2.9	–0.4	–25.7	0.7	28.0	99.7	7.72
Minimum	53.0	0.6	26	66	–8.0	–3.1	–29.7	0.0	24.2	75.8	0.08
Catoche											
n	19	19	19	19	42	42	21	21	21	20	19
Average	81.1	18.9	85	220	–8.5	–1.6	–28.6	0.1	27.0	93.6	1.36
Standard deviation	20.1	20.1	46	155	0.8	0.9	1.7	0.2	2.3	6.3	1.61
Maximum	98.9	47.1	178	420	–6.7	0.0	–26.4	0.9	35.0	99.7	4.66
Minimum	52.9	1.1	31	33	–11.2	–3.2	–35.0	0.0	23.8	76.4	0.08
Boat Harbour											
n	26	26	26	26	50	50	30	30	28	29	26
Average	83.3	16.7	204	236	–6.8	–2.3	–26.2	0.6	23.9	92.4	1.22
Standard deviation	12.8	12.8	162	105	0.9	0.7	2.4	0.6	2.4	5.2	1.19
Maximum	99.4	31.5	715	479	–4.0	–0.9	–22.1	2.7	32.6	98.8	4.01
Minimum	68.5	0.6	38	98	–8.5	–4.2	–35.1	0.1	19.7	75.2	0.09
Watts Bight											
n	16	16	16	16	23	23	15	15	15	15	16
Average	74.6	25.4	75	196	–8.2	–1.3	–26.8	0.8	25.8	92.7	0.74
Standard deviation	19.3	19.3	33	120	1.4	0.4	1.8	0.7	1.6	13.0	0.70
Maximum	99.1	45.8	158	390	–6.0	–0.6	–22.2	3.3	28.2	99.1	2.32
Minimum	54.2	0.9	35	27	–11.3	–2.2	–28.6	0.1	22.2	46.1	0.09

Note: VPDB, Vienna PeeDee Belemnite.

Fig. 3. A scatter diagram of Mn/Sr versus (*a*) $\delta^{13}C$ and (*b*) $\delta^{18}O$ for the micritic lime mudstone and dolomicrite from the investigated sequences, showing no correlation.

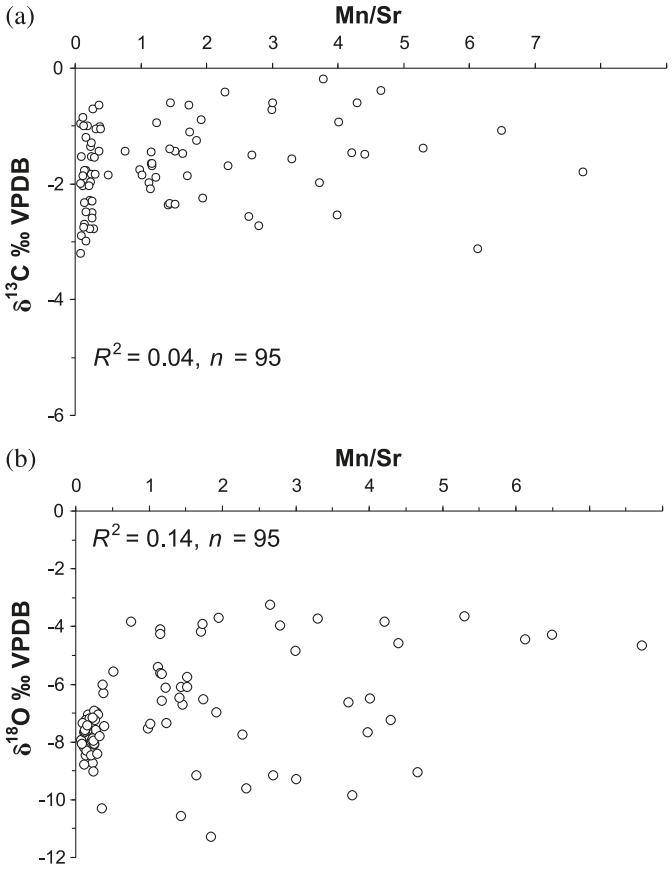

Fig. 4. Oxygen- versus carbon-isotope values for the investigated carbonates, showing insignificant correlations.

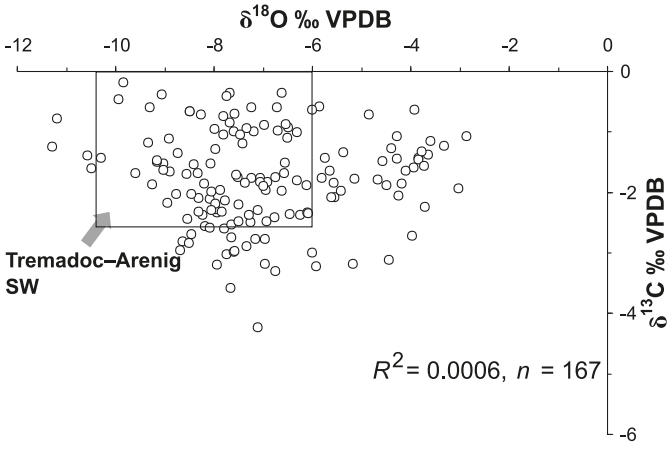

cycle of Knight and James 1987). Multiple-stage dolomitization is relatively abundant in the St. George group carbonates (Knight et al. 2007, 2008; Azmy et al. 2008).

The biostratigraphic framework of the St. George Group has been studied and refined by several authors (e.g., Williams et al. 1987; Boyce and Stouge 1997; Boyce et al. 2000; Zhang and Barnes 2004 and references therein) and is summarized in Fig. 2. The sea-level changes (Fig. 2) reconstructed from the conodont biozonation (cf. Zhang and Barnes 2004) cover the upper St. George Group between the uppermost Boat Harbour Formation (Barbace Cove Member) and the lowermost part of the Table Point Formation (Table Head Group) immediately overlying the Aguathuna Formation. However, no reliable reconstructions are known yet to cover the lower part of the St. George Group from the middle member of the Boat Harbour Formation down to the base of Watts Bight Formation (Fig. 2).

The sea-level curve exhibits consistent rises of relatively fast flooding events (Fig. 2), which are correlated, in some cases, with few centimetre thick shale layers overlying thin beds of brecciated carbonates. On the other hand, the same curve shows a drop in sea level at the topmost part of the sequence associated with the regional St. George Unconformity.

Fig. 5. A scatter diagram of $\delta^{13}C$ versus the total organic carbon contents (TOC; %) in the studied carbonates.

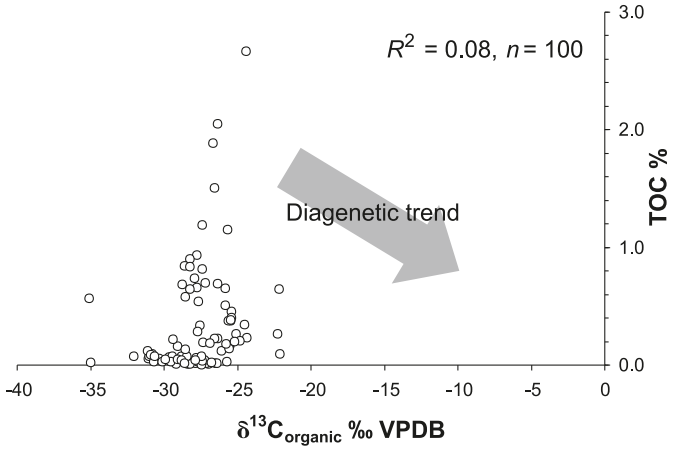

Fig. 6. The $\delta^{13}C$ values of St. George carbonates versus their carbonate contents.

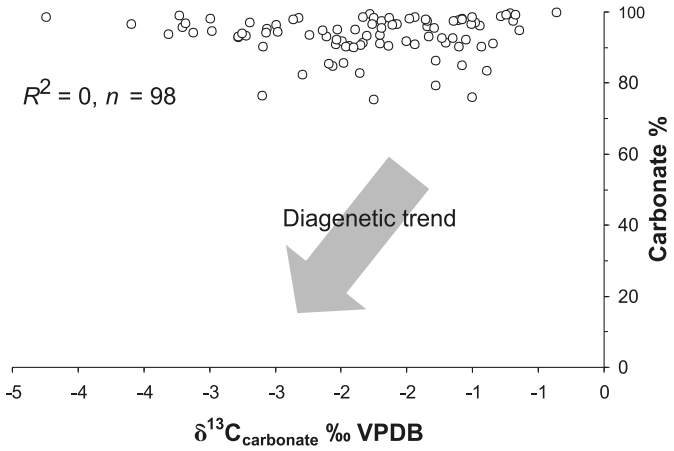

Methodology

Samples were collected at high resolution (sampling interval ≤2 m, Appendix A Table A1) from outcrops and cores (Fig. 1) from Port au Port Peninsula and from Port au Choix in western Newfoundland (cf. Knight et al. 2007, 2008; Azmy et al. 2008, 2009; Greene 2008; Conliffe et al. 2009; and more details available at the CISTI, Depository of

Fig. 7. Correlation of the $\delta^{13}C_{carb}$ and $\delta^{13}C_{org}$ profiles of the investigated St. George Group (current study) with the global $\delta^{13}C_{carb}$ (after Shields et al. 2003; Bergström et al. 2009). The broken line on the global $\delta^{13}C_{carb}$ profile represents the mean values documented by Shields et al. (2003) and the width of the grey band represents the $\pm 2\sigma$ values, whereas the thick black line represents the global values compiled by Bergström et al. (2009) from Buggisch et al. (2003) and Kaljo et al. (2007). The numerical age estimates and chronostratigraphic divisions follow the global scheme after Gradstein et al. (2004) and Bergström et al. (2009). Numbered bars refer to the conodont biozonation scheme as in Fig. 2 and arrows next to letters along the $\delta^{13}C_{carb}$ profile point at the most significant events. Legend as in Fig. 2.

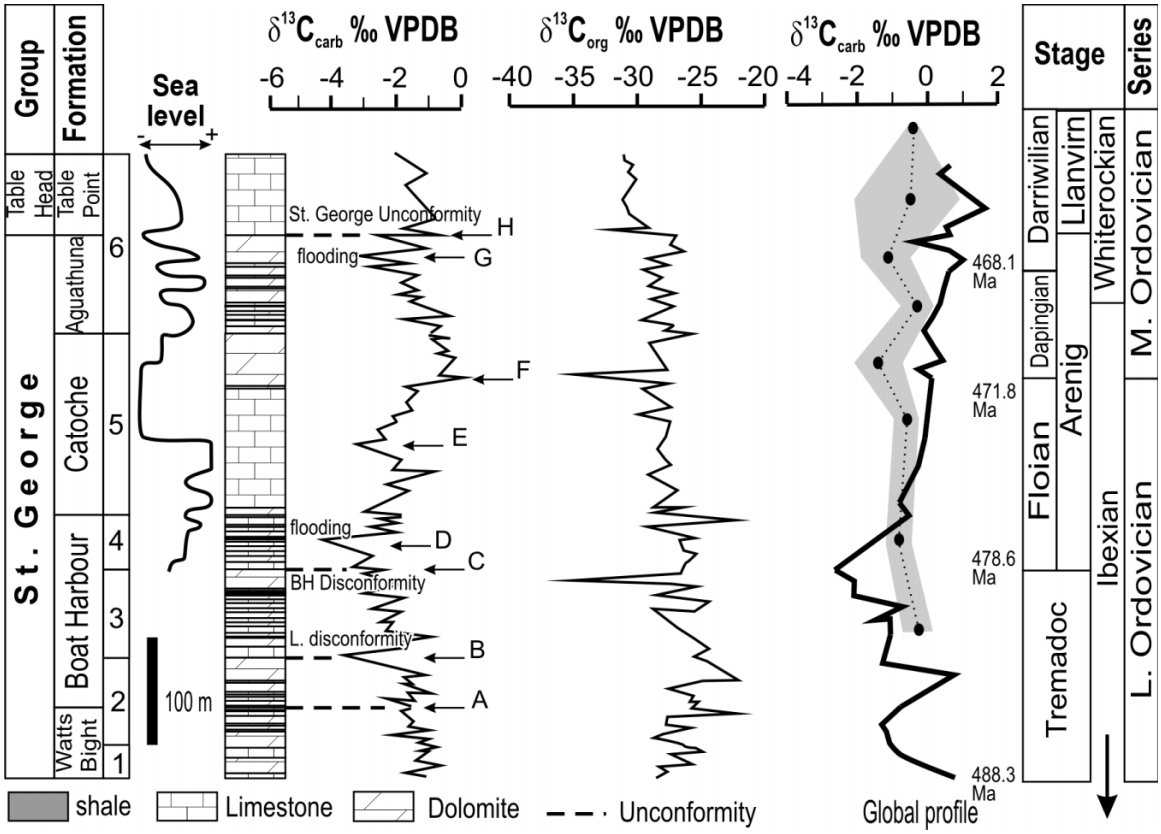

Unpublished Data). The locations of the sampled outcrops and cores are shown in Fig. 1, and the details of the covered intervals with the stratigraphic levels from which the samples were collected are provided in Table A1. The sampled outcrops and cores were carefully selected to cover the maximum thickness of the formations and to avoid tectonic complications.

Thin sections of the samples were examined petrographically with a polarizing microscope and cathodoluminoscope and stained with Alizarin Red-S and potassium ferricyanide solutions. A mirror-image slab of each thin section was also prepared and polished for microsampling. Cathodoluminescence observations were performed using an ELM-3R cold cathode instrument operated at ~12 kV accelerating voltage and ~0.7 mA gun current intensity.

Polished slabs were washed with deionized water and dried overnight at 50 °C prior to the isolation of the finest grained micritic lime mudstone and dolomicrites free of cements. Approximately 5 mg were microsampled from the nonluminescent lime mudstone and dolomicrite in cleaned slabs with a low-speed microdrill under a binocular microscope. The geochemical analyses have been mainly carried out on the microsampled carbonate, except for those of the evaluation of carbonate contents and the measurements of $\delta^{13}C$ of organic carbon that were run on bulk sample powders.

For C- and O-isotope analyses, ~220 μg of powder sample was reacted in inert atmosphere with ultrapure-concentrated (100%) orthophosphoric acid at 70 °C in a Thermo-Finnigan Gasbench II and the produced CO_2 was automatically delivered to the source of a Thermo-Finnigan DELTA V plus isotope ratio mass spectrometer in a stream of helium, where the gas was ionized and measured for isotope ratios. Uncertainties of better than 0.1‰ (2σ) for the analyses were determined by repeated measurements of NBS-19 ($\delta^{18}O$ = –2.20‰ and $\delta^{13}C$ = +1.95‰ versus Vienna PeeDee Belemnite (VPDB)) and L-SVECS ($\delta^{18}O$ = –26.64‰ and $\delta^{13}C$ = –46.48‰ versus VPDB), as well as internal standards.

For elemental analyses, a subset of sample powder was digested in 5% (*v*/*v*) acetic acid for 70–80 min and analyzed for Ca, Mg, Sr, and Mn (Coleman et al. 1989) using a HP 4500^{plus} at Memorial University of Newfoundland, St. John's, Newfoundland. The relative uncertainties of these measurements are better than 5%. Calculations are based on 100% carbonates.

Organic carbon isotope ratios were measured on isolated kerogen, after repeated treatment with concentrated hydrochloric acid at the isotope laboratory of Memorial University of Newfoundland, using a Carlo Erba Elemental Analyzer coupled to a 252 Finnigan MAT mass spectrometer. The re-

sults were normalized to the standards IAEA-CH-6 ($\delta^{13}C$ = –10.43‰), NBS18 ($\delta^{13}C$ = –5.04‰), and USGS24 ($\delta^{13}C$ = –15.99‰); and the uncertainty calculated from repeated measurements was ~0.2‰.

Results and discussion

The geochemical attributes of the St. George Group carbonates are described in detail in Table A1 and their statistics are summarized in Table 2. The chemostratigraphic correlations are mainly based on the distinctive variations in the $\delta^{13}C_{carb}$ profile of the investigated sequences, which exhibit the $\delta^{13}C_{carb}$ variations in preserved micritic carbonates. These variations may reflect environmental or diagenetic perturbations (Table A1). Therefore, the evaluation of the retained geochemical signatures is a cornerstone for the reconstructions of reliable chemostratigraphic profiles.

Evaluation of sample preservation

Several petrographic and geochemical techniques have been utilized to evaluate the degree of preservation of the studied Lower Ordovician micritic carbonates of the St. George Group (e.g., Azmy et al. 2006). Thin sections were examined using a petrographic microscope for grain size, degree of recrystallization, detrital components, and sedimentary structures. The St. George micritic carbonates exhibit insignificant recrystallization and preservation of primary sedimentary fabrics (e.g., Azmy et al. 2008, 2009). This is also true for many of the dolomitized horizons likely because dolomitization has started at very early stages of diagenesis.

Cathodoluminescence was utilized to study the diagenetic and depositional components and to refine the selection of best preserved carbonates (e.g., Azmy et al. 2001, 2006). Luminescence in carbonates is mainly activated by high concentrations of Mn and quenched by high concentrations of Fe (Machel and Burton 1991). Bright luminescence indicates diagenetic alteration; but the degree of carbonate luminescence, however, may have to be taken with caution because some altered carbonates might still exhibit no luminescence due to high Fe contents (Rush and Chafetz 1990).

The trace element analyses of the current investigations were obtained from microsamples, which were drilled from the finest grained carbonates. The Mn and Sr abundances and $\delta^{18}O$ of carbonates are significantly modified by alteration under the influence of diagenetic fluids, which results in significant enrichment in Mn contents but depletions in those of Sr and ^{18}O (Brand and Veizer 1980; Veizer 1983). Therefore, the Mn/Sr ratio of marine carbonates is commonly utilized as a tool for evaluating their degree of preservation (e.g., Derry et al. 1992; Kaufman and Knoll 1995). In general, ratios up to 10 (low Sr contents) have been accepted for $\delta^{13}C_{carb}$ studies particularly because the diagenetic fluids, at low water–rock interaction associated with insignificant recrystallization, do not have much CO_2 to reset the C-isotopic composition of the carbonates (e.g., Kaufman and Knoll 1995; Corsetti and Kaufman 2003).

The Mn/Sr ratios of the investigated dolomicrite and lime mudstones of the St. George Group range from ~0.1 to 7.7 (1.38 ± 1.69, n = 95; Table 2) and Sr concentrations reach up to ~653 ppm (220 ± 130 ppm, n = 95; Table 2). Some of the lime mudstones may still retain high Sr contents (>600 ppm) comparable with those of modern marine carbonates (cf. Brand et al. 2003) and thus suggesting a local high degree of preservation. Therefore, the $\delta^{13}C$ values of most samples may be considered as little altered given the lack of relationship of Sr contents with Mn/Sr ratios (Fig. 3*a*).

Oxygen-isotope compositions of carbonates are also sensitive monitors of alteration by diagenetic fluids, which are usually ^{18}O-depleted relative to seawater. However, the preservation of dominant micritic grain size and retention of sedimentary fabrics of the investigated carbonates may argue against severe diagenetic alteration. Although the $\delta^{18}O$ values range widely from –11.3‰ to –2.9‰ VPDB (Fig. 3*b*), suggesting variable degrees of alteration, there is no systematic relationship between the Mn/Sr and $\delta^{18}O$ (Fig. 3*b*) or between the $\delta^{18}O$ and $\delta^{13}C$ values (Fig. 4). Also, it is noteworthy that the majority of the $\delta^{13}C$ values of the microsampled micritic limemuds and dolomicrites fall within the documented range of the well-preserved carbonates deposited from the Early to Middle Ordovician seawaters (Veizer et al. 1999; Shields et al. 2003), thus suggesting high degree of preservation of chemical signatures (Fig. 4). The lack of petrographic evidence for significant recrystallization (cf. Banner and Hanson 1990), the absence of any correlation between $\delta^{13}C$ and Mn/Sr values, the comparable $\delta^{13}C$ values obtained from micritic limestones and dolomicrites from the same layer, and the consistency of $\delta^{13}C$ values in closely spaced stratigraphic samples (Table A1) support the view that the variations in the $\delta^{13}C$ values of the St. George Group carbonates may reflect depositional conditions (cf. Kaufman and Knoll 1995; Azmy et al. 2001, 2006).

The $\delta^{13}C_{org}$ values of organic matter (Table 2), isolated from selected samples (Fig. 5), range from ca. ~–35‰ to –22.1‰ (–27.6‰ ± 2.2‰, n = 100). The Taconian and Acadian deformation affecting western Newfoundland might have resulted in efficient plumbing systems for channelizing very high-temperature fluid flows, which could have led to some metamorphic enrichment of the $\delta^{13}C_{org}$ in organic matter (cf. Schidlowski et al. 1975; Hayes et al. 1983, 1999) and affected the $\delta^{13}C_{carb}$. However, the lack of correlation between the $\delta^{13}C_{org}$ and total organic carbon (TOC) abundance in the studied carbonates (Fig. 5) would argue against any metamorphic influence (e.g., Azmy et al. 2006). The lack of correlation between the $\delta^{13}C_{carb}$ values and carbonate abundance in bulk samples (Fig. 6) also argues against the influence of any terrestrial input of organic matter on the C-isotope composition of carbonates.

The absence of abundant bacterial pyrite, pipelike sedimentary structure, or significant depletion in the $\delta^{13}C$ of the analyzed micritic carbonates dismisses the potential diagenetic influence of the sulfate reducing zone and methanogenesis on the $\delta^{13}C$ signatures of the studied carbonates (e.g., Patterson and Walter 1994; Dickson et al. 2008). Variations in the value of the $\delta^{13}C$ excursions in a profile can be influenced by the absolute depth of the epiric seas and the locations of sediment relative to open ocean water due to effect of significance of circulation (e.g., Immenhauser et al. 2008), but the occurrence of some shelly fossils (e.g., brachiopod shell fractions) in the investigated carbonates agues for insignificant variations in water depth.

St. George Group $\delta^{13}C$ isotope stratigraphy

Petrographic observations and geochemical results indicate that the $\delta^{13}C$ signatures of the investigated St. George Group carbonates are preserved or at least near primary. Thus, the constructed $\delta^{13}C$ stratigraphic profiles are reliable and depict temporal variations in Early–Middle Ordovician seawater chemistry (Fig. 7).

The $\delta^{13}C_{carb}$ profile of the St. George Group carbonates (Fig. 7) reveals some significant negative isotopic excursions, which vary between ~1.5‰ and 3.0‰. These shifts are correlated with unconformities–disconformities (sea-level lowstands) or thin shale interbeds (interpreted as flooding surfaces), thus reflecting the effect of considerable sea-level changes on the $\delta^{13}C$ ratios of carbonates. Long-term stratification of oceans (e.g., Zhang et al. 2001) results in shut down of effective oceanic circulation and nutrient flux (e.g., Hotinski et al. 2001; Hoffman and Schrag 2002), which may also develop dramatic depletions in the $\delta^{13}C$ composition of carbonates. However, the St. George carbonates exhibit no evidence to support such scenario.

The Watts Bight – Boat Harbour formation boundary is marked by an erosion surface; and there are two disconformities within the Boat Harbour Formation itself (Fig. 7), the lower disconformity and the upper Boat Harbour Disconformity (Knight et al. 2008; Azmy et al. 2009; Conliffe et al. 2009). In the upper part of the formation, a ~2 cm thick shale interbed occurs and is interpreted to have resulted from a brief and rapid sea-level rise (Knight et al. 2008). The C-isotope compositions of the Boat Harbour carbonates (–2.3‰ ± 0.7‰ VPDB, n = 50; Table 2) are generally depleted relative to those of the underlying Watts Bight carbonates (–1.3‰ ± 0.4‰ VPDB, n = 23; Table 2). The $\delta^{13}C_{carb}$ profile of the Watts Bight Formation shows generally no significant excursions (Fig. 7) and no significant $\delta^{13}C_{carb}$ variation has been recorded at the Watts Bight – Boat Harbour unconformable boundary (A, Fig. 7). This might suggest that the time hiatus physically was possibly small and involved no significant variations in the seawater carbon budget.

On the contrary, the Boat Harbour $\delta^{13}C_{carb}$ profile has two negative shifts, one correlated with each of the disconformities, but the shift of the lower disconformity (B, Fig. 7) is larger (~3‰) than that of the Boat Harbour Diconformity (C, ~1.5‰; Fig. 7). Also, a remarkable depletion (~10‰) followed by quick recovery in the $\delta^{13}C_{org}$ in sediments occurs at a stratigraphic level immediately below the Boat Harbour Disconformity (C, Fig. 7) and is correlated with a high $\delta^{13}C_{carb}$ value, suggesting a short episode of considerable high organic productivity before the sea-level drop. The drop in sea level, which resulted in the unconformity, might have possibly brought oxygen-rich shallow seawater in contact with organic matter buried and (or) induced the migration of unconformity-related lowstand lens of oxygenated waters in the shallow buried sediments that oxidized organic matter to release ^{12}C-rich bicarbonate ions (cf. Holmden et al. 1998; Immenhauser et al. 2008).

The Barbace Cove sediments that overly the Boat Habour Disconformity have been suggested by earlier studies (e.g., Knight and James 1987) to be deposited by a eustatic early Arenigian rise. However, the incomplete sea-level reconstructions covering the time of the Boat Harbour – Watts Bight interval make it difficult at this stage to speculate on the global extension of the lower Boat Harbour Disconformity sea-level fall.

A third negative $\delta^{13}C_{carb}$ shift (D, ~2.2‰; Fig. 7) found in the uppermost section (Barbace Cove Member) of the Boat Harbour Formation is correlated with a thin shale layer (~2 cm thick; Knight et al. 2008) overlying a thin bed of brecciated carbonates (minor sedimentary hiatus). A steadily and significant increase in $\delta^{13}C_{carb}$ ratios is observed for carbonates that overly the Boat Harbour Formation (Fig. 7). The Catoche Formation carbonates have generally more enriched $\delta^{13}C_{carb}$ values (–1.6‰ ± 0.9‰ VPDB, n = 42; Table 2) compared with their underlying Boat Harbour counterparts (–2.3‰ ± 0.7‰ VPDB, n = 50; Table 2), which might reflect a general increase in organic primary productivity in the basin. Unlike the Boat Harbour, the Catoche $\delta^{13}C_{carb}$ profile exhibits only one significant negative $\delta^{13}C_{carb}$ excursion (E, ~3.2‰; Fig. 7) spanning roughly the middle interval of the formation. This shift is correlated with the end of sea-level highstand and the beginning of dramatic sea-level fall (Zhang and Barnes 2004), which is physically expressed in transition from low-energy muddy carbonate lithofacies to high-energy grainstones (Knight et al. 2007; Greene 2008). The lack of a correlated response on the $\delta^{13}C_{org}$ profile makes hard to speculate on the mechanism that caused the $\delta^{13}C_{carb}$ depletion. On the other hand, sea-level reconstructions (Zhang and Barnes 2004) show a long period of lowstand during most of the upper part of the Catoche Formation with sea-level rise only recorded in the topmost part of the formation (Fig. 7). The $\delta^{13}C_{carb}$ profile shows also a positive shift of ~3‰ (F, Fig. 7) towards the topmost part of the formation, which occurs at the end of a long-term but slow-paced increase in $\delta^{13}C_{carb}$ (Fig. 7). The positive $\delta^{13}C_{carb}$ peak (F) is correlated with a significant negative $\delta^{13}C_{org}$ shift of ~8‰ (Fig. 7). This may suggest a recovery of the marine biota and organic productivity during the overall lowstand and a final acceleration of recovery at the onset of significant flooding over the Catoche peritidal platform leading to more burial of organic carbon (Fig. 7). This is also consistent with the general enrichment in the $\delta^{13}C_{carb}$ compositions of the Catoche Formation carbonates relative to their underlying counterparts (Table 2).

The Aguathuna Formation carbonates have comparable C-isotope composition (–1.5‰ ± 0.6‰ VPDB, n = 50; Table 2) to that of the underlying Catoche carbonates (–1.6‰ ± 0.9‰ VPDB, n = 42; Table 2). However, the general $\delta^{13}C_{carb}$ profile of the Aguathuna carbonates is part of a long-term decreasing trend that started in the upper part of the Catoche Formation, but the values never get to the very negative ratios yielded by the lower units of the St. George (Fig. 7). The Aguathuna $\delta^{13}C_{carb}$ profile has two major negative shifts (Fig. 7), one near the top of the formation (G) and the other one that coincides with the level of the regional St. George Unconformity (H), which marks the Aguathuna – Table Point formation boundary (Knight et al. 2007). The near-top negative shift (G, ~2‰; Fig. 7) is associated with a minor disconformity overlain by a thin (few centimetre thick) transgressive shale bed, whereas the topmost boundary shift (H, ~2‰; Fig. 7) is correlated with a major sea-level fall during the St. George Unconformity (Fig. 7). The St. George Unconformity is characterized by major subaerial exposure

that led to meteoric diagenesis and significant karstification of the topmost rocks of the formation (Lane 1990; Knight et al. 1991, 2007; Azmy et al. 2008). The St. George Unconformity negative $\delta^{13}C_{carb}$ shift also correlates with a positive $\delta^{13}C_{org}$ shift of ~5‰ (Fig. 7), thus likely reflecting the effect of oxidation of organic matter during sea-level fall, which brought oxygen-rich shallow seawater and (or) lowstand meteoric water lenses in contact with buried organic matter, which resulted in release of ^{12}C-rich CO_2 (cf. Holmden et al. 1998; Immenhauser et al. 2008).

Implications for global correlations

Age uncertainty and low resolution of the global biostratigraphic framework are amongst the main reasons for problems in stable isotope global correlations and paleooceanographic models. The current study uses the most up-to-date Early and Middle Ordovician international classifications (Tremadocian, Floian, Dapingian, and Darriwilian; Gradstein et al. 2004; Bergström et al. 2009) alongside the previously used British (Tremadocian, Arenigian, and Llanvirnian) and North American (Ibexian and Whiterockian) stratigraphic stage nomenclatures (cf. Shields et al. 2003; Knight et al. 2007, 2008) in attempt to refine, if possible, the global correlation of the investigated St. George Group sequence (Fig. 7).

The C-isotope compositions of Lower Ordovician carbonates have been investigated in other sedimentary basins (e.g., Holmden et al. 1998; Buggisch et al. 2003; Shields et al. 2003; Kaljo et al. 2007; Bergström et al. 2009) on different landmasses. The global Early Ordovician $\delta^{13}C_{carb}$ profile (Bergström et al. 2009 and more references therein) has been mainly reconstructed from complete dataset obtained from basins in Argentina (Buggisch et al. 2003) and Baltoscandia (Kaljo et al. 2007).

Although the sedimentological evidences suggest deposition in warm shallow marine water (epiric seas), the $\delta^{13}C_{carb}$ composition of the St. George Group carbonates (~–4‰ to +1‰ VPDB) is slightly lighter than that (~–3‰ to +2‰ VPDB) of the Argentinean and Baltoscandian counterparts (Fig. 7). The petrographic and geochemical criteria of the investigated rocks support high degree of preservation, which dismisses the potential influence of diagenetic alteration. Variations in carbon cycling in sedimentary basins, organic activity, circulation, and distance from open water conditions have been known to play a significant role in controlling the $\delta^{13}C_{carb}$ of marine carbonates (Azmy et al. 1998; Kump and Arthur 1999; Holmden et al. 1998; Veizer et al. 1999; Immenhauser et al. 2008). Sediments of the inner epiric environment are deposited in water masses of little exchanges with open sea compared with those deposited in more outward settings closer to open-water marine circulation and exchanges. This may influence the input of nutrients and organic matter through terrestrial input and also upwelling, which will likely control the $\delta^{13}C_{carb}$ values (e.g., Holmden et al. 1998; Calver 2000; Immenhauser et al. 2008). Also, expansion and contraction of epicontinental water masses (e.g., sea-level changes) by local tectonic activities might result in some variable $\delta^{13}C_{carb}$ excursions in the C-isotope profile of a particular sedimentary basin despite the absence of global-scale changes in the Earth's ocean system during that time (e.g., Holmden et al. 1998).

The profile shows negative shifts (Fig. 7), each of ~2‰, which are possibly comparable to those on the St. George profile. The global mid-Tremadocian shift can be correlated with the negative shift (B) on the local profile and with the lower Boat Harbour Disconformity. Also, the global shift at the Tremadocian–Floian boundary can be correlated to the local shift (D), taking into consideration the uncertainty in the stratigraphic position of the biozone boundaries. On the other hand, a global positive $\delta^{13}C_{carb}$ excursion (~3.5‰) reaches its maximium around the Floian–Dapingian boundary and can be correlated the positive shift (F) on the St. George profile (~4‰; Fig. 7).

The St. George Group $\delta^{13}C_{carb}$ profile shows several negative excursions (A–H, Fig. 7) that are herein correlated with sea-level changes along the Laurentian margin. Although sea-level reconstructions for the Early Ordovician from eastern Laurentia (Zhang and Barnes 2004), Baltic region, and central Australia (Nielsen 1992*a*, 1992*b*) exhibit slight differences (cf. Zhang and Barnes 2004), they all agree on a major sea-level lowstand near the end of Arenig. Along the paleosouthern margin of Laurentia, this unconformity (with local nomenclature) extends from southeastern USA (Mussman and Read 1986) to southern Quebec (Salad Hersi et al. 2007; Lavoie et al. in press) to Anticosti (Desrochers et al. in press) and as far as eastern Greenland (Boyce and Stouge 1997; Knight et al. 2007). At the large scale, the global negative $\delta^{13}C_{carb}$ shift around the lowermost Darriwilian (uppermost Arenig) coincides biostratigraphically with the St. George Unconformity in western Newfoundland and its associated negative $\delta^{13}C_{carb}$ shift (H, ~2‰; Fig. 7). This is also consistent with the profile of Shields et al. (2003), which is based on data from Utah and Oklahoma. However, it has shown that the development of the lower Middle Ordovician unconformity in western Newfoundland (Knight et al. 1991) and its nearby areas (Salad Hersi et al. 2007) had a significant tectonic component related to ongoing subduction in the Iapetus Ocean near Laurentia. Very fine-scale, combined palynology and $\delta^{13}C_{carb}$ studies could eventually generate data on fine-scale diachroneity of the isotopic shift and epilogue on the tectonic–eustatic relative contributions to the development of the unconformity and related isotopic shift.

In summary, although the local $\delta^{13}C_{carb}$ profile of western Newfoundland has several excursions, only a few of them can be potentially correlated with comparable shifts on the global counterpart. The remaining excursions are most likely local and related to changes in the depositional environment of the western Newfoundland Lower–Middle Ordovician platform at the margin of Laurentia.

Conclusions

Petrographic and geochemical investigations of samples collected at high resolution from outcrops and cores covering the St. George Group carbonates suggest high degree of confidence in preservation of near-marine pristine $\delta^{13}C$ signatures.

The St. George Group $\delta^{13}C_{carb}$ profile exhibits negative excursions, which are correlated with variations in the sea-level fluctuations and in the $\delta^{13}C_{org}$ values of the coeval kerogen.

The sea-level reconstructions from Laurentia, Baltica, and central Australia exhibit a major sea-level lowstand around the end of Arenig, which is stratigraphically correlated with the regional St. George Unconformity. The unconformity is associated with a negative $\delta^{13}C_{carb}$ excursion in the Aguathuna Formation carbonates (St. George Group) that matches a global negative $\delta^{13}C_{carb}$ shift. Even if the St. George Unconformity in western Newfoundland has a significant tectonic component, it possibly also records a global sea-level lowstand.

The St. George Group $\delta^{13}C_{carb}$ profile has other excursions around the mid-Tremadoc, Late Tremadoc, and middle Arenig, which can be correlated with similar shifts on the global profile. However, correlations with global excursions have to be taken with cautions, since local environmental changes (e.g., tectonism) might also result in similar excursions. Additional geochemical studies on the St. George Group carbonates from other locations in western Newfoundland will certainly provide more conclusive constraints on this issue.

Acknowledgement

The authors wish to thank Dr. Brian Pratt and an anonymous reviewer for their constructive reviews. Also, efforts of Drs. George Dix (*Associate Editor*) and John Greenough (*Editor*) are much appreciated. This project was supported by funding (to Karem Azmy) from the Earth Science Sector of Natural Resources Canada (NRCan), the Pan-Atlantic Petroleum Systems Consortium (PPSC), and the Irish Shelf Petroleum Studies Group (ISGSP).

References

Azmy, K., Veizer, J., Misi, R., De Olivia, T., Sanches, A.L., and Dardenne, M. 2001. Isotope stratigraphy of the neoproterozoic carbonate of vazante formation Saõ Francisco Basin, Brazil. Precambrian Research, **112**: 303–329. doi:10.1016/S0301-9268(01)00194-2.

Azmy, K., Kaufman, A.J., Misi, A., and Oliveira, T.F. 2006. Isotope stratigraphy of the Lapa Formation, São Francisco Basin, Brazil: Implications for Late Neoproterozoic glacial events in South America. Precambrian Research, **149**(3–4): 231–248. doi:10.1016/j.precamres.2006.07.001.

Azmy, K., Lavoie, D., Knight, I., and Chi, G. 2008. Dolomitization of the Aguathuna Carbonates in Western Newfoundland, Canada: implications for a potential hydrocarbon reservoir. Canadian Journal of Earth Sciences, **45**(7): 795–813. doi:10.1139/E08-020.

Azmy, K., Lavoie, D., Knight, I., and Chi, G. 2009. Origin of Boat Harbour dolomites of the St. George Group in western Newfoundland, Canada: implications for porosity development. Bulletin of Canadian Petroleum Geology, **57**: 1–24.

Baker, D., and Knight, I. 1993. The Catoche dolomite project, Anticosti Basin, eastern Canada. Centre for Earth Resources Research (CERR) Report, Memorial University of Newfoundland, St. John's, Nfld. 174 p.

Banner, J.L., and Hanson, G.N. 1990. Calculations of simultaneous isotopic and trace element variations during water–rock interaction with applications to carbonate diagenesis. Geochimica et Cosmochimica Acta, **54**(11): 3123–3137. doi:10.1016/0016-7037(90)90128-8.

Bergström, S.M., Chen, X., Gutiérrez-Marco, J.C., and Dronov, A. 2009. The new chronostratigraphic classification of the Ordovician System and its relations to major regional series and stages and to $\delta^{13}C$ chemostratigraphy. Lethaia, **42**(1): 97–107. doi:10.1111/j.1502-3931.2008.00136.x.

Boyce, W.D. 1989. Early Ordovician trilobite faunas of the Boat Harbour and Catoche formations (St. George Group) in the Boat Harbour – Cape Norman area, Great Northern Peninsula, western Newfoundland. Newfoundland Department of Mines and Energy, Report 89-2, 169 p.

Boyce, W.D., and Stouge, S. 1997. Trilobite and conodont biostratigraphy of the St. George Group, Eddies Cove West area, western Newfoundland. Newfoundland Department of Mines and Energy, Report 91-1, pp. 183–200.

Boyce, W.D., Knight, I., Rohr, D.M., Williams, S.H., and Measures, E.A. 2000. The upper St. George Group, western Port au Port Peninsula: lithostratigraphy, biostratigraphy, depositional environments and regional implications. Current Research 2000. Newfoundland Department of Mines and Energy, Geological Survey Report 2000-1, pp. 101–125.

Brand, U., Logan, A., Hiller, N., and Richardson, J. 2003. Geochemistry of modern brachiopods: applications and implications for oceanography and paleoceanography. Chemical Geology, **198**(3–4): 305–334. doi:10.1016/S0009-2541(03)00032-9.

Brand, U., and Veizer, J. 1980. Chemical diagenesis of a multicomponent carbonate system: 1. Trace elements. Journal of Sedimentary Petrology, **50**: 1219–1236.

Buggisch, W., Keller, M., and Lehnert, O. 2003. Carbon isotope record of late Cambrian to Early Ordovician carbonates of the Argentine Precordillera. Palaeogeography, Palaeoclimatology, Palaeoecology, **195**(3–4): 357–373. doi:10.1016/S0031-0182(03)00365-1.

Cawood, P.A., McCausland, P.J.A., and Dunning, G.R. 2001. Opening Iapetus: Constraints from Laurentian margin in Newfoundland. Geological Society of America Bulletin, **113**(4): 443–453. doi:10.1130/0016-7606(2001)113<0443:OICFTL>2.0.CO;2.

Calver, C.R. 2000. Isotope stratigraphy of the Ediacarian (Neoproterozoic III) of the Adelaide Rift Complex, Australia, and the overprint of water column stratification. Precambrian Research, **100**(1–3): 121–150. doi:10.1016/S0301-9268(99)00072-8.

Chi, G., and Ni, P. 2007. Equations for calculation of NaCl/(NaCl+$CaCl_2$) ratios and salinities from hydrohalite-melting and ice-melting temperatures in the H_2O–NaCl–$CaCl_2$ system. Acta Petrolei Sinica, **23**: 33–37.

Coleman, M.L., Walsh, J.N., and Benmore, R.A. 1989. Determination of both chemical and stable isotope composition in milligram-size carbonate samples. Sedimentary Geology, **65**(3–4): 233–238. doi:10.1016/0037-0738(89)90025-0.

Conliffe, J., Azmy, K., Knight, I., and Lavoie, D. 2009. Dolomitization in the Lower Ordovician Watts Bight Formation of the St Georges Group, western Newfoundland. Canadian Journal of Earth Sciences, **46**: 247–261. doi:10.1139/E09-019.

Cooper, M., Weissenberger, J., Knight, I., Hostad, D., Gillespie, D., Williams, H., et al. 2001. Basin evolution in western Newfoundland: New insights from hydrocarbon exploration. The American Association of Petroleum Geologists Bulletin, **85**: 393–418.

Corsetti, F.A., and Kaufman, A.J. 2003. Stratigraphic investigations of carbon isotope anomalies and Neoproterozoic ice ages in Death Valley, California. Geological Society of America Bulletin, **115**: 916–932. doi:10.1130/B25066.1.

Derry, L.A., Kaufman, A.J., and Jacobsen, S.B. 1992. Sedimentary cycles and environmental change in the Late Proterozoic: evidence from stable and radiogenic isotopes. Geochimica et Cosmochimica Acta, **56**(3): 1317–1329. doi:10.1016/0016-7037(92)90064-P.

Desrochers, A., Lavoie, D., Brennan-Alpert, P., and Chi, G. Regional stratigraphic, depositional and diagenetic patterns from the interior of St. Lawrence Platform: the Lower Ordovician Romaine Formation, western Anticosti Basin, Québec. *In* The Great American Bank. *Edited by* J. Derby. American Association of Petroleum Geologist, Memoir, in press.

Dickson, J.A.D., Wood, R.A., Bu Al Rougha, H., and Shebl, H. 2008. Sulphate reduction associated with hardgrounds: lithification afterburn! Sedimentary Geology, **205**(1–2): 34–39. doi:10.1016/j.sedgeo.2008.01.005.

Gradstein, F.M., Ogg, J.G., Smith, A.G., Bleeker, W., and Lourens, L.J. 2004. A new Geologic Time Scale, with special reference to Precambrian and Neogene. Episodes, **27**: 83–100.

Greene, M. 2008. Multiple generations of dolomitization in the Catoche Formation, Port au Choix, Newfoundland. M.Sc. thesis, Memorial University of Newfoundland, St. John's, Nfld., 146 p.

Halverson, G.P., Hoffman, P.F., Schrag, D.P., Maloof, A.C., and Rice, A.H.N. 2005. Toward a Neoproterozoic composite carbon-isotope record. Geological Society of America Bulletin, **117**(9): 1181–1207. doi:10.1130/B25630.1.

Hayes, J.M., Kaplan, I.R., and Wedeking, K.W. 1983. Precambrian organic geochemistry; preservation of the record. *In* Earth's earliest biosphere; its origin and evolution. *Edited by* J. Schopf. Princeton University Press, Princeton, N.J., pp. 93–134.

Hayes, J.M., Strauss, H., and Kaufman, A.J. 1999. The abundance of ^{13}C in marine organic matter and isotopic fractionation in the global biogeochemical cycle of carbon during the past 800 Ma. Chemical Geology, **161**(1–3): 103–125. doi:10.1016/S0009-2541(99)00083-2.

Hoffman, P.F., and Schrag, D.P. 2002. The Snowball Earth hypothesis: testing the limits of global change. Terra Nova, **14**(3): 129–155. doi:10.1046/j.1365-3121.2002.00408.x.

Holmden, C., Creaser, R.A., Muehlenbachs, K., Leslie, S.A., and Bergström, S.M. 1998. Isotopic evidence for geochemical decoupling between ancient epeiric seas and bordering oceans: Implications for secular curves. Geology, **26**(6): 567–570. doi:10.1130/0091-7613(1998)026<0567:IEFGDB>2.3.CO;2.

Hotinski, R.M., Bice, K.L., Kump, L.R., Najjar, R.G., and Arthur, M.A. 2001. Ocean stagnation and end-Permian anoxia. Geology, **29**(1): 7–10. doi:10.1130/0091-7613(2001)029<0007:OSAEPA>2.0.CO;2.

Immenhauser, I., Holmden, C., and Patterson, W.P. 2008. Interpreting the carbon-isotope record of ancient shallow epiric seas: lessons from the Recent. Geological Association of Canada, Special Paper 48, pp. 137–174.

Jacobi, R.D. 1981. Peripheral bulge — a causal mechanism for the Lower I Middle Ordovician unconformity along the western margin of the northern Appalachians. Earth and Planetary Science Letters, **56**: 245–251. doi:10.1016/0012-821X(81)90131-X.

Ji, Z., and Barnes, C.R. 1993. A major conodont extinction event during the Early Ordovician within the Midcontinent Realm. Palaeogeography, Palaeoclimatology, Palaeoecology, **104**(1–4): 37–47. doi:10.1016/0031-0182(93)90118-3.

James, N.P., Stevens, R.K., Barnes, C.R., and Knight, I. 1989. Evolution of a Lower Paleozoic continental-margin carbonate platform, northern Canadian Appalachians. *In* Controls on Carbonate Platform and Basin Development. *Edited by* P.D. Crevello, J.L. Wilson, J.F. Sarg, and J.F. Read. Society of Economic Paleontologists and Mineralogists, Special Publication 44, pp. 123–146.

Kaljo, D., Martma, T., and Saadre, T. 2007. Post-Hunnebergian Ordovician carbon isotope trend in Baltoscandia, itsenvironmental implications and some similarities with that of Nevada. Palaeogeography, Palaeoclimatology, Palaeoecology, **245**(1–2): 138–155. doi:10.1016/j.palaeo.2006.02.020.

Kaufman, A.J., and Knoll, A.H. 1995. Neoproterozic variations in the C-isotopic composition of seawater: stratigraphic and biogeochemical implications. Precambrian Research, **73**(1–4): 27–49. doi:10.1016/0301-9268(94)00070-8.

Knight, I. 1991. Geology of Cambro-Ordovician rocks in the Port Saunders (NTS 12I/11), Castors River (NTS12I/15), St. John Island (NTS 12I/14) and Torrent River (NTS 121/10) map areas. *Edited by* R.F. Blackwood, C.P.G. Pereira, and D.G. Walsh. Newfoundland Department of Mines and Energy, Mineral Development Division, Report 91-4, 138 p.

Knight, I., and James, N.P. 1987. The stratigraphy of the Lower Ordovician St. George Group, western Newfoundland: the interaction between eustasy and tectonics. Canadian Journal of Earth Sciences, **24**: 1927–1952. doi:10.1139/e87-185.

Knight, I., James, N.P., and Lane, T.E. 1991. The Ordovician St. George Unconformity, northern Appalcachians: the relationship of plate convergence at the St. Lawrence Promontory to the Sauk/Tippecanoe sequence boundary. Geological Society of America Bulletin, **103**(9): 1200–1225. doi:10.1130/0016-7606(1991)103<1200:TOSGUN>2.3.CO;2.

Knight, I., Azmy, K., Greene, M., and Lavoie, D. 2007. Lithostratigraphic setting of diagenetic, isotopic, and geochemistry studies of Ibexian and Whiterockian carbonates of the St. George and Table Head groups in western Newfoundland. Current Research Newfoundland and Labrador Department of Natural Resources Geological Survey. Report 07-1, pp. 55–84.

Knight, I., Azmy, K., Boyce, D., and Lavoie, D. 2008. Tremadocian carbonates of the lower St. George Group, Port au Port Peninsula, western Newfoundland: Lithostratigraphic setting of diagenetic, isotopic, and geochemistry studies. Current Research Newfoundland and Labrador Department of Natural Resources Geological Survey. Report 08-1, pp. 1–43.

Kump, L.R., and Arthur, M.A. 1999. Interpreting carbon-isotope excursions: carbonates and organic matter. Chemical Geology, **161**(1–3): 181–198. doi:10.1016/S0009-2541(99)00086-8.

Lane, T.E. 1990. Dolomitization, brecciation and zinc mineralization and their paragenetic, stratigraphic and structural relationships in the upper St. George Group (Ordovician) at Daniel's Harbour, western Newfoundland: Unpublished Ph.D. thesis, Memorial University of Newfoundland, St. John's, Nfld., 496 p.

Lavoie, D. 1994. Diachronous tectonic collapse of the Ordovician continental margin, eastern Canada: comparison between the Quebec Reentrant and the St. Lawrence Promontory. Canadian Journal of Earth Sciences, **31**: 1309–1319. doi:10.1139/e94-113.

Lavoie, D., Desrochers, A., Dix, G.R., Knight, I., and Salad Hersi, O. The Great American Carbonate Bank (GACB) in eastern Canada — An overview. *In* The Great American Bank. *Edited by* J. Derby. American Association of Petroleum Geologist, Memoir, in press.

Machel, H.G., and Burton, E.A. 1991. Factors governing cathodoluminescence in calcite and doloomite, and their implications for studies of carbonate diagenesis. *In* Luminescence microscopy and spectroscopy, qualitative and quantitative applications. (SEPM) Short Course, **25**: 37–57.

Mussman, W.J., and Read, J.G. 1986. Sedimentology and development of a passive- to convert-margin unconformity: Middle Ordovician Knox Unconformity, Virginia Appalachians. Geological Society of America Bulletin, **97**(3): 282–295. doi:10.1130/0016-7606(1986)97<282:SADOAP>2.0.CO;2.

Nielsen, A.T. 1992*a*. Ecostratigraphy and the recognition of Arenigian (Early Ordovician) sea-level changes. *In* Global perspectives on Ordovician geology. *Edited by* B.D. Webby and J.R.

Laurie. A.A. Balkema, Rotterdam, the Netherlands, pp. 355–366.

Nielsen, A.T. 1992*b*. International correlation of the Arenigian (Early Ordovician) based on sequence and ecostratigraphy. *In* Global perspectives on Ordovician geology. *Edited by* B.D. Webby and J.R. Laurie. A.A. Balkema, Rotterdam, the Netherlands, pp. 367–379.

Patterson, W.P., and Walter, L.M. 1994. Depletion of ^{13}C in seawater SCO_2 on modern carbonate platforms: significance for the carbon isotopic record of carbonates. Geology, **22**: 885–888.

Pratt, B.R., and James, N.P. 1986. The tidal flat island model for peritidal shallow-upward sequences; St. George Group, western Newfoundland. Sedimentology, **33**: 313–344.

Qing, H., and Veizer, J. 1994. Oxygen and carbon isotopic composition of Ordovician brachiopods: Implications for coeval seawater. Geochimica et Cosmochimica Acta, **58**(20): 4429–4442. doi:10.1016/0016-7037(94)90345-X.

Rush, P.F., and Chafetz, H.S. 1990. Fabric retentive, nonluminescent brachiopods as indicators of original $\delta^{13}C$ and $\delta^{18}O$ compositions: a test. Journal of Sedimentary Petrology, **60**: 968–981.

Salad Hersi, O., Nowlan, G.S., and Lavoie, D. 2007. A revision of the stratigraphic nomenclature of the Cambrian–Ordovician strata of the Philipsburg tectonic slice, southern Québec. Canadian Journal of Earth Sciences, **44**(12): 1775–1790. doi:10.1139/E07-041.

Schidlowski, M., Eichmann, R., and Junge, C.E. 1975. Precambrian sedimentary carbonates: carbon and oxygen isotope geochemistry and implications for the terrestrial oxygen budget. Precambrian Research, **2**(1): 1–69. doi:10.1016/0301-9268(75)90018-2.

Shields, G.A., Carden, G.A.F., Veizer, J., Meidla, T., Rong, J.-Y., and Li, R.-Y. 2003. Sr, C, and O isotope geochemistry of Ordovician brachiopods: a major isotopic event around the Middle–Late Ordovician transition. Geochimica et Cosmochimica Acta, **67**(11): 2005–2025. doi:10.1016/S0016-7037(02)01116-X.

Smith, M.P. 1991. Early Ordovician conodonts of East and North Greenland. Meddelelser om Grønland Geoscience. Vol. 26, 81 p.

Stenzel, S.R., Knight, I., and James, N.P. 1990. Carbonate platform to foreland basin: revised stratigraphy of the Table Head Group (Middle Ordovician), western Newfoundland. Canadian Journal of Earth Sciences, **27**(1): 14–26. doi:10.1139/e90-002.

Stouge, S., Boyce, W.D., Christiansen, J.L., Harper, D.A.T., and Knight, I. 2001. Lower–Middle Ordovician stratigraphy of North-East Greenland. Geology of Greenland Survey Bulletin, **189**: 107–114.

Stouge, S., Boyce, W.D., Christiansen, J.L., Harper, D.A.T., and Knight, I. 2002. Vendian–Lower Ordovician stratigraphy of Ella Ø North-East Greenland: new investigation. Geology of Greenland Survey Bulletin, **191**: 117–125.

Veizer, J. 1983. Chemical diagenesis of carbonates. *In* Theory and application of trace element technique. *Edited by* M.A. Arthur, T.F. Anderson, I.R. Kaplan, J. Veizer, and L.S. Land. Stable Isotopes in Sedimentary Geology. Society of Economic Paleontologists and Mineralogists (SEPM), Short course notes 10: III-1–III-100.

Veizer, J., Ala, D., Azmy, K., Bruckschen, P., Bruhn, F., Buhl, D., et al. 1999. $^{87}Sr/^{86}Sr$, $\delta^{18}O$ and $\delta^{13}C$ evolution of Phanerozoic seawater. Chemical Geology, **161**(1–3): 59–88. doi:10.1016/S0009-2541(99)00081-9.

Williams, S.H., Boyce, W.D., and James, N.P. 1987. Graptolites from the Lower–Middle Ordovician St. George and Table Head groups, western Newfoundland, and their correlation with trilobite, graptolite, brachiopod and conodont zones. Canadian Journal of Earth Sciences, **24**: 456–470. doi:10.1139/e87-047.

Wilson, J.L., Medlock, P.L., Fritz, R.D., Canter, K.L., and Geesaman, R.G. 1992. A review of Cambro-Ordovician breccias in North America. *In* Paleokarst, karst-related diagenesis and reservoir development. *Edited by* M.P. Candelaria and C.L. Reed. SEPM-Permian Basin Section, Publication 92-33, pp. 19–29.

Zhang, S., and Barnes, C.R. 2004. Arenigian (Early Ordovician) sea-level history and the response of conodont communities, western Newfoundland. Canadian Journal of Earth Sciences, **41**(7): 843–865. doi:10.1139/e04-036.

Zhang, R., Follows, M.J., Grotzinger, J.P., and Marshall, J. 2001. Could the Late Permian deep ocean have been anoxic? Paleoceanagraphy, **16**(3): 317–329. doi:10.1029/2000PA000522.

Appendix A

Table A1 appears on the following pages.

Table A1. Samples, description, and elemental and stable isotopic geochemical compositions of the investigated carbonates.

Sample No.	Formation	Outcrop/Core	Sample level (m)	Phase	$CaCO_3$%
R1-004	Table Point (top)	Core RND1	4	C1	
R1-010	Table Point	Core RND1	10	C1	94.5
R1-016	Table Point	Core RND1	16	C1	92.1
R1-022	Table Point	Core RND1	22	C1	94.6
R1-028	Table Point	Core RND1	28	C1	96.2
R1-034	Table Point	Core RND1	34	C1	95.6
R1-041	Table Point	Core RND1	41	C1	93.5
R1-047	Table Point	Core RND1	47	C1	69.8
R1-053	Table Point	Core RND1	53	C1	93.9
R1-059	Table Point	Core RND1	59	C1	
R1-065	Table Point	Core RND1	65	C1	96.8
R1-071	Table Point	Core RND1	71	C1	92.3
R1-075	Table Point	Core RND1	75	C1	97.1
R1-079	Table Point (base)	Core RND1	79	C1	
KAR1-081	Aguathuna (top)	Core RND1	81	D1	55.7
KAR1-083	Aguathuna	Core RND1	83	D1	
KAR1-085	Aguathuna	Core RND1	85	D1	55.4
KAR1-087	Aguathuna	Core RND1	87	D1	
KAR1-089	Aguathuna	Core RND1	89	D1	55.0
KAR1-091	Aguathuna	Core RND1	91	D1	
KAR1-093	Aguathuna	Core RND1	93	D1	54.8
KAR1-095	Aguathuna	Core RND1	95	D1	
KAR1-099	Aguathuna	Core RND1	99	D1	56.1
KAR1-102	Aguathuna	Core RND1	102	D1	53.0
KAR1-106	Aguathuna	Core RND1	106	D1	55.8
KAR1-108	Aguathuna	Core RND1	108	D1	
KAR1-110	Aguathuna	Core RND1	110	C1	99.2
KAR1-112	Aguathuna	Core RND1	112	C1	95.0
KAR1-118	Aguathuna	Core RND1	118	D1	
KAR1-120	Aguathuna	Core RND1	120	D1	56.5
KAR1-122	Aguathuna	Core RND1	122	D1	55.5
KAR1-124	Aguathuna	Core RND1	124	C1	99.4
KAR1-128	Aguathuna	Core RND1	128	D1	
KAR1-130	Aguathuna	Core RND1	130	D1	55.1
KAR1-132	Aguathuna	Core RND1	132	D1	
KAR1-134	Aguathuna	Core RND1	134	D1	
KAR1-136	Aguathuna	Core RND1	136	C1	99.3
KAR1-138	Aguathuna	Core RND1	138	D1	
KAR1-142	Aguathuna	Core RND1	142	D1	54.7
KAR1-144	Aguathuna	Core RND1	144	D1	54.9
KAR1-146	Aguathuna	Core RND1	146	D1	
KAR1-148	Aguathuna	Core RND1	148	D1	
KAR1-150	Aguathuna	Core RND1	150	D1	58.3
KAR1-154	Aguathuna	Core RND1	154	C1	
KAR1-160	Aguathuna	Core RND1	160	C1	97.4
KAR1-162	Aguathuna	Core RND1	162	D1	55.3
KAR1-164	Aguathuna	Core RND1	164	D1	55.1
KAR1-166	Aguathuna	Core RND1	166	C1	99.2
KAR1-168	Aguathuna	Core RND1	168	C1	99.4
KAR1-172	Aguathuna	Core RND1	172	C1	98.3
KAR1-174	Aguathuna	Core RND1	174	C1	
KAR1-176	Aguathuna (base)	Core RND1	176	C1	
49	Catoche-Costa Bay Mbr. Dolomite (top)	Core PC79-02	44.1	D1	55.6
44	Catoche-Costa Bay Mbr. Dolomite	Core PC79-02	37.5	D1	61.0
40	Catoche-Costa Bay Mbr. Dolomite	Core PC79-02	33.5	D1	55.0
37	Catoche-Costa Bay Mbr. Dolomite	Core PC79-02	30.5	D1	
31	Catoche-Costa Bay Mbr. Dolomite	Core PC79-02	24.5	D1	54.6

$MgCO_3$%	Mn (ppm)	Sr (ppm)	$\delta^{18}O$ ‰ VPDB	$\delta^{13}C$ carbonate ‰ VPDB	$\delta^{13}C$ organic ‰ VPDB	TOC %	$\Delta\delta$	Carbonate %
			–6.2	–2.0	–31.1	0.05	29.0	90.9
5.5	559	340	–6.3	–1.5	–31.0	0.07	29.5	91.8
7.9	712	325	–5.4	–1.2	–30.3	0.05	29.1	91.3
5.4	336	379	–6.6	–1.1	–30.7	0.02	29.6	98.0
3.8	164	367	–6.1	–1.1	–30.1	0.03	29.0	97.5
4.4	150	396	–6.5	–1.7	–30.8	0.09	29.1	91.0
6.5	230	393	–6.0	–1.3				
30.2	135	286	–5.0	–1.3	–31.1	0.12	29.8	86.2
6.1	66	380	–6.3	–1.2	–30.9	0.09	29.7	92.6
			–6.1	–1.1	–30.6	0.07	29.5	97.4
3.2	58	231	–6.1	–0.8				
7.7	108	269	–6.1	–1.3	–29.2	0.02	27.8	95.9
2.9	160	329	–6.6	–1.8	–32.0	0.07	30.3	99.3
			–7.0	–0.7	–27.5	0.01	26.9	97.5
44.3	239	90	–3.2	–2.6	–26.9	0.01	24.4	95.2
			–3.5	–2.4				
44.6	177	91	–3.7	–2.2	–26.5	0.01	24.2	93.4
			–3.9	–1.6	–27.4	0.01	25.9	96.6
45.0	149	87	–4.2	–1.9				
			–2.9	–1.1	–26.4	0.01	25.3	97.8
45.2	70	92	–3.8	–1.4	–27.0	0.01	25.5	98.6
			–4.2	–2.1	–28.1	0.02	26.1	84.7
43.9	585	96	–4.4	–3.1	–29.2	0.02	26.0	94.0
47.0	741	96	–4.7	–1.8				
44.2	120	104	–4.1	–1.6	–27.6	0.01	25.9	90.3
			–4.5	–1.9				
0.8	58	204	–7.0	–2.8	–29.5	0.04	26.8	92.7
5.0	109	653	–7.1	–1.8				
			–5.4	–1.3	–28.1	0.02	26.7	97.4
43.5	346	79	–4.6	–1.5				
44.5	320	76	–3.8	–1.5				
0.6	45	182	–6.9	–1.8	–29.1	0.02	27.3	98.4
			–5.1	–1.8				
44.9	348	66	–3.7	–1.4				
			–3.8	–1.3	–27.0	0.02	25.7	93.0
			–3.0	–1.9	–27.8	0.06	25.9	90.4
0.7	48	355	–7.2	–1.8				
			–3.3	–1.2	–28.8	0.07	27.6	92.5
45.3	237	72	–3.7	–1.6	–27.1	0.02	25.6	96.4
45.1	126	109	–4.3	–1.5				
			–4.4	–1.3	–27.2	0.04	25.9	79.2
			–3.6	–1.2				
41.7	836	129	–4.3	–1.1	–27.9	0.02	26.9	84.9
			–6.6	–0.4	–28.4	0.00	28.0	99.7
2.6	229	232	–7.5	–1.8	–29.7	0.07	27.9	98.3
44.7	219	73	–4.8	–0.7				
44.9	202	117	–3.9	–0.6	–27.2	0.69	26.5	94.7
0.8	26	312	–8.0	–1.0				
0.6	69	254	–7.6	–0.7	–27.8	0.02	27.1	99.5
1.7	39	208	–7.2	–1.0	–25.7	0.03	24.7	75.8
			–7.7	–0.4				
			–5.9	–0.6				
44.4	122	63	–7.0	–0.9	–29.1	0.16	28.2	83.4
39.0	159	37	–7.2	–0.6				
45.0	116	51	–7.7	–0.4				
			–8.3	–0.7				
45.4	124	33	–9.8	–0.2				

Table A1 (*continued*).

Sample No.	Formation	Outcrop/Core	Sample level (m)	Phase	$CaCO_3$%
27	Catoche-Costa Bay Mbr. Dolomite	Core PC79-02	18.5	D1	60.8
22	Catoche-Costa Bay Mbr. Dolomite	Core PC79-02	13.5	D1	
20	Catoche-Costa Bay Mbr. Dolomite	Core PC79-02	11.5	D1	
17	Catoche-Costa Bay Mbr. Dolomite	Core PC79-02	6.5	D1	
15	Catoche-Costa Bay Mbr. Dolomite	Core PC79-02	6.5	D1	
13	Catoche-Costa Bay Mbr. Dolomite	Core PC79-02	4.5	D1	
11	Catoche-Costa Bay Mbr. Dolomite	Core PC79-02	2.5	D1	61.1
10	Catoche-Costa Bay Mbr. Dolomite	Core PC79-02	1.5	D1	
9	Catoche-Costa Bay Mbr. Dolomite (base)	Core PC79-02	0.4	D1	52.9
131	Catoche (top)	Outcrop	120	D1	
130	Catoche	Outcrop	119	C1	98.6
129	Catoche	Outcrop	111	C1	93.6
128	Catoche	Outcrop	107	C1	
127	Catoche	Outcrop	102	C1	
126	Catoche	Outcrop	98	D1	65.8
125	Catoche	Outcrop	95	C1	94.9
124	Catoche	Outcrop	92	C1	
123	Catoche	Outcrop	89	C1	98.9
120	Catoche	Outcrop	82	C1	
119	Catoche	Outcrop	77	C1	
118	Catoche	Outcrop	71	C1	
117	Catoche	Outcrop	67	C1	98.5
116	Catoche	Outcrop	62	C1	
115	Catoche	Outcrop	57	C1	97.8
114	Catoche	Outcrop	55	C1	
113	Catoche	Outcrop	50	C1	98.5
111	Catoche	Outcrop	43	D1	
110	Catoche	Outcrop	41	C1	97.1
109	Catoche	Outcrop	35	C1	
108	Catoche	Outcrop	30	C1	98.5
107	Catoche	Outcrop	25	C1	
106	Catoche	Outcrop	12	C1	98.7
105	Catoche	Outcrop	8	C1	
104	Catoche	Outcrop	5	C1	
103	Catoche	Outcrop	4	C1	98.7
102	Catoche	Outcrop	4	C1	
100	Catoche (base)	Outcrop	1	C1	
BH67 (top)	Boat Harbour	Outcrop	174	C1	97.1
BH66	Boat Harbour	Outcrop	172	C1	99.4
BH64	Boat Harbour	Outcrop	168	C1	
BH62	Boat Harbour	Outcrop	165	C1	98.8
BH60	Boat Harbour	Outcrop	161	D1	
BH58	Boat Harbour	Outcrop	158	D1	77.5
BH56	Boat Harbour	Outcrop	154	C1	
BH55	Boat Harbour	Outcrop	152	C1	
BH53	Boat Harbour	Outcrop	148	D1	
BH51	Boat Harbour	Outcrop	144.5	C1	
BH50	Boat Harbour	Outcrop	142	D1	
BH49	Boat Harbour	Outcrop	141	C1	
BH47	Boat Harbour	Outcrop	138	C1	
BH45	Boat Harbour	Outcrop	135	D1	72.4
BH43	Boat Harbour	Outcrop	130	C1	99.0
BH41	Boat Harbour	Outcrop	126	D1	
BH40	Boat Harbour	Outcrop	125	D1-C1	79.3
BH38b	Boat Harbour	Outcrop	122	D1	71.5
BH37	Boat Harbour	Outcrop	120	C1	99.2

$MgCO_3$%	Mn (ppm)	Sr (ppm)	$\delta^{18}O$ ‰ VPDB	$\delta^{13}C$ carbonate ‰ VPDB	$\delta^{13}C$ organic ‰ VPDB	TOC %	$\Delta\delta$	Carbonate %
39.2	155	33	–9.1	–0.4				
			–8.5	–0.7	–27.7	0.03	27.0	99.1
			–8.5	0.0	–35.0	0.02	35.0	99.4
			–8.5	–0.7	–27.5	0.00	26.8	
			–8.5	0.0	–28.2	0.00	28.3	99.7
			–9.9	–0.5				
38.9	100	33	–9.3	–0.6	–29.2	0.01	28.6	
			–11.2	–0.8				98.7
47.1	97	66	–6.7	–0.6				
			–8.6	–1.7	–29.4	0.07	27.7	93.4
1.4	68	291	–8.7	–1.4	–29.5	0.03	28.2	97.9
6.4	70	293	–9.0	–1.5				
			–8.9	–1.7				
			–8.3	–1.7	–27.4	0.03	25.7	97.4
34.2	178	66	–9.2	–1.5				
5.1	40	363	–8.8	–2.0	–29.9	0.05	27.8	94.9
			–8.1	–2.1	–28.6	0.04	26.5	93.0
1.1	33	391	–8.0	–2.0	–27.5	0.07	25.5	91.6
			–8.2	–2.4				
			–8.2	–2.6	–27.8	0.93	25.2	94.1
			–7.9	–2.3				
1.5	31	405	–7.9	–3.2	–28.4	0.07	25.2	95.6
			–8.6	–2.8				
2.2	47	336	–8.5	–2.7	–27.8	0.04	25.1	97.0
			–8.9	–2.2				
1.5	33	291	–8.2	–1.9	–27.3	0.19	25.5	82.6
			–8.3	–2.1				
2.9	50	420	–7.7	–0.8	–29.1	0.04	28.2	91.1
			–7.5	–2.2				
1.5	71	326	–8.0	–2.3				
			–9.0	–1.6	–26.8	0.02	25.1	98.3
1.3	82	352	–7.9	–2.0	–28.8	0.04	26.8	90.1
			–7.8	–2.6	–26.4	0.22	23.8	76.4
			–8.5	–2.4				
1.3	47	326	–8.3	–2.3	–28.6	0.01	26.3	98.3
			–8.7	–3.0				
			–9.3	–1.9				
2.9	148	479	–7.1	–1.8	–25.1	0.26		91.3
0.6	65	250	–7.3	–2.5	–22.2	0.64	19.7	96.3
			–7.0	–2.0				
1.2	87	384	–7.2	–2.8	–29.4	0.22	26.6	93.0
			–6.3	–2.4				
22.5	715	193	–6.6	–2.0	–25.4	0.38	23.5	85.5
			–6.0	–3.0	–26.6	1.50		
			–7.1	–4.2	–26.7	1.88	22.4	98.5
			–5.9	–3.2	–26.4	2.05	23.1	98.8
			–7.7	–3.0				
			–5.2	–3.2	–25.4	0.45	22.2	96.8
			–7.0	–3.2				
			–8.5	–2.8				
27.6	306	110	–4.0	–2.7	–26.1	0.12	23.4	93.2
1.0	38	419	–7.3	–2.9				
			–6.7	–3.3	–26.6	0.22	23.3	93.7
20.7	391	98	–7.7	–2.5				
28.5	182	128	–6.5	–2.4	–28.2	0.90	25.9	97.9
0.8	62	380	–7.6	–3.0	–27.4	1.19	24.4	98.0

Table A1 (*continued*).

Sample No.	Formation	Outcrop/Core	Sample level (m)	Phase	$CaCO_3$%
BH36	Boat Harbour	Outcrop	118	D1	
BH35	Boat Harbour	Outcrop	116	D1	
BH34	Boat Harbour	Outcrop	114	D1	
BH33	Boat Harbour	Outcrop	112.5	D1	
BH32	Boat Harbour	Outcrop	110	D1	76.4
BH30	Boat Harbour	Outcrop	106	D1	75.0
BH28	Boat Harbour	Outcrop	102	C1	
BH26	Boat Harbour	Outcrop	98	D1	
BH24	Boat Harbour	Outcrop	94	D1	74.3
BH22	Boat Harbour	Outcrop	89.5	C1	98.7
BH20	Boat Harbour	Outcrop	85.5	D1	74.4
BH18	Boat Harbour	Outcrop	82	D1	69.5
BH16	Boat Harbour	Outcrop	78	C1	98.8
BH14	Boat Harbour	Outcrop	74	D1	72.6
BH12	Boat Harbour	Outcrop	68.5	D1	
BH10	Boat Harbour	Outcrop	64.5	C1	
BH08	Boat Harbour	Outcrop	61	D1	72.2
BH06	Boat Harbour	Outcrop	56	C1	
BH04	Boat Harbour	Outcrop	52	C1	
BH02	Boat Harbour	Outcrop	48	C1	99.2
BH-A23	Boat Harbour	Outcrop	44	C1	
BH-A17	Boat Harbour	Outcrop	30	D1	76.9
BH-A15	Boat Harbour	Outcrop	25.5	D1	72.4
BH-A14	Boat Harbour	Outcrop	24	C1	
BH-A11	Boat Harbour	Outcrop	19	D1	
BH-A09	Boat Harbour	Outcrop	15	D1	
BH-A07-2	Boat Harbour	Outcrop	11	D1	69.4
BH-A05	Boat Harbour	Outcrop	8	C1	75.6
BH-A03	Boat Harbour	Outcrop	3	D1	68.5
BH-A02	Boat Harbour	Outcrop	2	C1	99.1
BH-A01 (base)	Boat Harbour	Outcrop	0.5	C1	99.2
WB30 (top)	Watts Bight	Outcrop	68	C1	98.5
WB29	Watts Bight	Outcrop	66		
WB28	Watts Bight	Outcrop	63		
WB27	Watts Bight	Outcrop	61.5		
WB26	Watts Bight	Outcrop	60	C1	99.1
WB25	Watts Bight	Outcrop	59	D1	64.3
WB24	Watts Bight	Outcrop	57		
WB23	Watts Bight	Outcrop	55		
WB22	Watts Bight	Outcrop	58	D1	54.2
WB21	Watts Bight	Outcrop	57		
WB20	Watts Bight	Outcrop	54		
WB19	Watts Bight	Outcrop	52		
WB18	Watts Bight	Outcrop	50.5	D1	54.8
WB17	Watts Bight	Outcrop	48		
WB16	Watts Bight	Outcrop	46	D1	
WB15A	Watts Bight	Outcrop	43.5	D1	97.0
WB14	Watts Bight	Outcrop	42	D1	
WB13	Watts Bight	Outcrop	40	D1	
WB12	Watts Bight	Outcrop	38	C1	
WB11	Watts Bight	Outcrop	36		
WB10	Watts Bight	Outcrop	34	D1	64.1
WB09	Watts Bight	Outcrop	32		
WB08	Watts Bight	Outcrop	30	C1	98.4
WB07	Watts Bight	Outcrop	27.5	D1	
WB06	Watts Bight	Outcrop	25	C1	

$MgCO_3$%	Mn (ppm)	Sr (ppm)	$\delta^{18}O$ ‰ VPDB	$\delta^{13}C$ carbonate ‰ VPDB	$\delta^{13}C$ organic ‰ VPDB	TOC %	$\Delta\delta$	Carbonate %
			–6.8	–2.4				
			–6.9	–2.5	–35.1	0.57	32.6	94.3
			–7.3	–2.4				
			–5.6	–2.1				
23.6	244	198	–6.1	–1.9	–25.4	0.40	23.5	95.0
25.0	270	187	–6.1	–2.3				
			–7.6	–3.0	–28.6	0.58	25.6	94.4
			–5.8	–1.8	–24.4	2.66	22.7	96.6
25.7	251	166	–6.1	–2.4				
1.3	47	357	–7.6	–2.8	–28.8	0.69	26.0	93.8
25.6	124	244	–5.6	–1.9	–25.5	0.16	23.7	90.6
30.5	141	126	–5.4	–2.0				
1.2	57	360	–7.5	–2.5				
27.4	240	209	–5.6	–2.1	–26.9	0.18	24.8	85.4
			–7.1	–2.3				
			–7.8	–2.3				
27.8	553	138	–6.5	–0.9	–25.6	0.16	24.6	90.3
			–8.0	–2.2				
			–7.0	–1.9	–24.4	0.23	22.5	90.0
0.8	62	242	–8.1	–2.6	–25.6	0.14	23.0	90.2
			–7.7	–3.6	–24.5	0.34	20.9	96.4
23.1	239	204	–6.6	–1.7				
27.6	304	175	–6.5	–1.1	–24.8	0.20	23.7	90.2
			–6.8	–1.8	–22.1	0.09	20.3	75.2
			–6.6	–1.5				
			–6.3	–1.8	–27.5	0.33	25.7	93.2
30.6	163	132	–7.3	–0.9	–25.6	0.38	24.7	96.0
24.4	276	236	–5.7	–1.7				
31.5	218	143	–5.7	–1.4	–25.8	0.51	24.4	90.9
0.9	78	304	–8.1	–2.3	–25.2	0.20	22.9	82.3
0.8	57	268	–8.5	–2.0	–25.7	0.18	23.7	92.1
1.5	70	239	–8.4	–1.5				
					–22.2	0.26	22.2	92.6
0.9	35	390	–8.1	–1.5				
35.7	158	156	–7.4	–1.8				
45.8	74	32	–9.6	–1.7	–27.7	0.28	26.0	95.3
45.2	67	41	–9.2	–1.5	–27.8	0.66	26.3	98.0
			–10.5	–1.6	–25.8	0.65	24.2	96.4
3.0	99	275	–7.6	–2.2				
			–6.7	–1.0	–27.9	0.73	27.0	97.0
			–8.9	–1.1				
			–7.8	–2.1	–28.6	0.84	26.5	94.8
35.9	96	257	–6.3	–1.0	–26.3	0.69	25.3	96.5
1.6	81	335	–8.0	–1.3	–25.4	0.38	24.1	95.4
			–6.5	–0.9				
			–7.8	–0.7	–24.7	3.28	24.0	99.1

Table A1 (*concluded*).

Sample No.	Formation	Outcrop/Core	Sample level (m)	Phase	$CaCO_3$%
WB05	Watts Bight	Outcrop	23	D1	60.2
WB04	Watts Bight	Outcrop	21.5	C1	99.1
WB03	Watts Bight	Outcrop	18.5	D1	
WB02	Watts Bight	Outcrop	16		
WB01	Watts Bight	Outcrop	14	D1	55.2
WB-A01	Burry Head	Outcrop	12		
WB-A03	Burry Head	Outcrop	10	D2	65.5
WB-A04	Burry Head	Outcrop	8	D1	62.1
WB-A05	Burry Head	Outcrop	6	D1	59.8
WB-A06	Burry Head	Outcrop	4.5	C1	98.3
WB-A07	Burry Head	Outcrop	1	C1	
WB-A08 (base)	Burry Head	Outcrop	0.1	C1	63.7

Note: C1 and D1 refer to micritic limestone and dolomicrite, respectively.

$MgCO_3$%	Mn (ppm)	Sr (ppm)	$\delta^{18}O$ ‰ VPDB	$\delta^{13}C$ carbonate ‰ VPDB	$\delta^{13}C$ organic ‰ VPDB	TOC %	$\Delta\delta$	Carbonate %
39.8	50	27	–11.3	–1.3				
0.9	42	341	–7.6	–1.0	–27.4	0.81	26.4	98.5
			–9.3	–1.2				
					–25.7	1.15	25.7	97.4
44.8	54	38	–10.6	–1.4				
					–28.2	0.65	28.2	94.9
34.5	130	145			–28.2	0.83	28.2	96.1
37.9	82	225	–6.0	–0.6				
40.2	45	142	–7.8	–1.1	–27.6	0.54	26.6	92.0
1.7	50	313	–7.4	–1.2				
			–7.5	–1.7	–28.6	0.13	26.8	46.1
36.3	69	175	–7.5	–1.1				